Energy Conversion and Management 258 (2022) 115378

Contents lists available at ScienceDirect

Energy Conversion and Management

journal homepage: www.elsevier.com/locate/enconman

Comprehensive experimental evaluation of R1234yf-based low GWP working fluids for refrigeration and heat pumps

Ali Khalid Shaker Al-Sayyab [a,b], Joaquín Navarro-Esbrí [a], Angel Barragán-Cervera [a], Sarah Kim [c], Adrián Mota-Babiloni [a,*]

[a] ISTENER Research Group, Department of Mechanical Engineering and Construction, Universitat Jaume I, Campus de Riu Sec s/n, 12071 Castelló de la Plana, Spain
[b] Basra Engineering Technical College (BETC), Southern Technical University, Basra, Iraq
[c] ARKEMA Inc, King of Prussia, PA, United States of America

ARTICLE INFO

Keywords:
Cooling and heating
Vapour compression system, global warming potential
R134a drop-in replacement
hydro-fluoro-olefines (HFO)
Energy efficiency

ABSTRACT

This work presents an experimental comparison for low GWP refrigerants used in vapour compression cooling and heating systems. The study compares three lower global warming potential (GWP) refrigerants (R513A, R516A, and R1234yf) as drop-in refrigerants to replace the hydrofluorocarbon (HFC) R134a. Measurements are taken from a test rig at different steady-state conditions: for the cooling mode, the evaporating temperature is −5 °C, −10 °C and −15 °C, and is combined with two condensing temperatures (32.5 °C and 40 °C), and different internal heat exchanger (IHX) effectiveness. Besides, in the heating mode, the evaporating temperature is 7.5, 15 and 22.5 °C with five condensing temperatures (55 °C to 75 °C, step of 5 °C). In the cooling mode, R513A presented the highest system COP amongst the low GWP alternatives, increasing up to 8%. R516A shows the lowest system COP at the highest evaporation temperature; however, it exhibits the highest COP and capacity at the lowest evaporation temperature. The IHX positively influences the refrigerating effect for all adopted refrigerants. Regarding the heating mode, R513A presents the highest heating capacity with an average 3% increase, whereas R516A shows the lowest results. R513A shows comparable COP to R134a, especially at higher evaporating temperatures.

1. Introduction

Global warming represents one of the most significant challenges humankind has faced in the last decades. In 2020, Europe was 1.2 °C warmer than the average year in the 19th Century [1]. In 2021, several countries suffered the highest temperature on record in Mediterranean basin countries and a higher number of fires than ever before [2]. Heat pump technology enables year-round comfort control for building occupants, domestic hot water, and district heating by extracting heat from ambient, water, ground, or industrial processes (waste heat recovery). The International Energy Agency 2050 technology roadmap recommends more efficient systems with simultaneous heating, cooling, and domestic hot water production [3].

In October 2016, the parties of the Montreal Protocol decided to accelerate their schedule to phase down HFCs. Developed countries, which ratify the Kigali Amendment to the Montreal Protocol, must reduce their HFCs consumption to 80% of their baseline by 2045 [4]. According to a recent strategy approved by Heat Roadmap Europe and the vision of the European Council's 20/20/20 target for reducing greenhouse gas emissions [5–6], it is essential to determine the carbon footprint of a heat pump system with low global warming potential (GWP) refrigerants. On the 27th of December 2020, the American Innovation and Manufacturing Act was enacted, which directs EPA to regulate and phase down production and consumption of HFCs to 15% of their baseline levels in a stepwise manner by 2036 [7].

One of the most commonly used HFC refrigerants is R134a, widely used in refrigeration, air conditioning, and heat pump applications [8].

Abbreviations: ASHRAE, The American Society of Heating, Refrigerating and Air-Conditioning Engineers; EES, Engineering Equation Solver; GHG, Greenhouse gas; GWP, Global warming potential; HFC, Hydrofluorocarbon; HFO, Hydro-fluoro-olefin; HP, Heat pump; IEA, International Energy Agency; IHX, Internal heat exchanger; LCCP, Life Cycle Climate Performance; ODP, Ozone depletion potential; On, With an internal heat exchanger; Off, Without an internal heat exchanger; PID, Proportional integral derivative; TEWI, Total equivalent warming Impact.

* Corresponding author.
E-mail addresses: alsayyab@uji.es, ali.alsayyab@stu.edu.iq (A.K.S. Al-Sayyab), navarroj@uji.es (J. Navarro-Esbrí), abarraga@uji.es (A. Barragán-Cervera), sarah.kim@arkema.com (S. Kim), mota@uji.es (A. Mota-Babiloni).

https://doi.org/10.1016/j.enconman.2022.115378
Received 14 November 2021; Received in revised form 10 February 2022; Accepted 11 February 2022
Available online 17 March 2022

Nomenclature

COP	Coefficient of performance (-)
E	annual electric energy consumption (kWh year^{-1})
h	Specific enthalpy (kJ kg^{-1})
L	leakage ratio (%)
$\dot{m}$	Refrigerant mass flow rate (kg s^{-1})
m	Refrigerant mass (kg)
NBP	Normal boiling point (°C)
n	lifetime of the heat pump system (years)
P	Pressure (MPa)
$\dot{Q}$	Heat transfer rate (kW)
q	Specific heat (kJ kg^{-1})
RPM	Revolution per minute
T	Temperature (°C)
$\dot{W}$	Electrical consumption power (kW)

Greek symbols

α	Refrigerant recovered (%)
β	Carbon emission factor (gCO_2-eq kWh^{-1})
Δ	Difference
ε	Heat exchanger effectiveness (-)
ρ	Refrigerant density (kg m^{-3})
v	Refrigerant specific volume (m^3 kg^{-1})
η	Efficiency (-)

Subscripts

C	Compressor; cooling
DS	Displacement
e	Evaporator
fg	vaporisation
H	Heating
IHX	Internal heat exchanger
is	Isentropic
k	Condenser
out	Outlet
s	Suction side of compressor conditions
v	Volumetric
w	Water
N	Normalized

It is a greenhouse gas (GHG), approximately 1400 times more potent than carbon dioxide. Phase-down and transition to working fluids with a GWP below 150 would mitigate the climate impact significantly caused by these widespread Refrigeration, heating ventilation, and air conditioning systems [9].

Hydrofluoroolefin (HFO) refrigerants are included in the fourth generation of fluorine-based refrigerants, potentially offering many of the benefits shown by HFCs but with a lower GWP. Owing to the olefinic structure, they have very short atmospheric lifetimes and have emerged as the best option for replacing high GWP HFCs. The first HFO, developed by DuPont and Honeywell, is R1234yf [10], presenting remarkably similar thermodynamic properties to R134a. Therefore, some authors consider it a straightforward replacement for R134a, with the only concern of its mild flammability.

Sethi et al. [11] theoretically simulated R1234yf and R1234ze(E) as drop-in refrigerants to R134a; they recommended minor design changes like modifying the heat exchanger circuiting and adding internal heat exchanger (IHX) to match the R134a energy performance. De Paula et al. [12] simulated heat pumps using R290, R1234yf, and R600a as an alternative refrigerant to R134a. The system with R290 shows higher system performance and is a promising alternative to R134a; its highly flammable nature must be considered. De Paula et al. [13] presented a simulation-optimisation study for a 1200 letter chilling unit using R744, R290, and R1234yf as R134a alternative refrigerants. The optimised system with R290 showed the highest energy and environmental performance. Janković et al. [14] experimentally studied R1234yf and R1234ze(E) as alternative refrigerants to R134a in small refrigeration units. R1234yf provided comparable performance to R134a; meanwhile, R1234ze(E) was required to increase the compressor size to match cooling capacity. In the same application, Sieres et al. [15] obtained an average R1234yf drop in cooling capacity and the energy efficiency rate by 6% and 8%, respectively. For domestic refrigerators, Li et al. [16] proved that R1234yf presents a comparable system performance to R134a and can be considered a drop-in alternative, whereas R600a showed the lowest system performance. Aprea et al. [17] demonstrated a 3% energy saving with R1234yf compared to R134a and improved cooling capacity. Gómez et al. [18] tested a 2.5 kW air to water cooling unit using R1234yf as a drop-in refrigerant to R134a. They concluded a 25% reduction in system performance using R1234yf. Colombo et al. [19] proved that R1234yf in a water-to-water heat pump shows a heating capacity and COP reduction up to 9.8% and 7.4%, respectively.

Other studies focused on using R1234yf as a drop-in refrigerant in automobile air conditioning systems with minor system components modifications. Lee et al. [20] experimentally observed that R1234yf cooling capacity reduction is down to 4%, with 2.7% system COP reduction. Cho et al. [21] optimised the incorporating an IHX with R1234yf; this component enhanced the system COP by 1.4%. Li et al. [22] experimentally proved that economiser vapour injection in the air conditioning system of electric vehicles with a 10% higher condenser size allows R1234yf to exceed the R134a heating capacity with a higher COP.

According to the ASHRAE safety classification, both R1234yf and R1234ze(E) are class A2L refrigerants, which indicates mildly flammability, representing one of the main barriers in their market expansion. Therefore, HFC/HFO mixtures have also been investigated as R134a drop-in replacements, offering a trade-off between flammability and GWP in such a way that the risk of the mixture would be lower than that of the single HFO refrigerant. However, based on the GWP, such blends would be considered intermediate solutions [23]. R1234yf and R1234ze (E) are components of new refrigerant mixtures like R450A, R513A, and R515A that aim to replace R134a in the short and medium-term with lower environmental impact. Many studies have already investigated these new refrigerant mixtures.

Meng et al. [24] experimentally studied automobile air conditioning units using a mixture of R1234yf/R134a (89/11 by mass percentage). The blend reduced R-134a COP in cooling and heating mode between 4% and 9% and 4% and 16%, respectively. For a small refrigeration system, Makhnatch et al. [25] experimental results showed that R513A provides comparable energy performance to R134a; meanwhile, R450A (58% R1234ze(E) and 42% R134a) showed system cooling capacity reduction. Also, in a refrigerator, Morales-Fuentes et al. [26] compared R513A (R1234yf/R134a 56/44 by mass percentage) and R1234yf as an alternative refrigerant to R134a, showing that R513A has a lower consumption power than R134a. However, both alternatives exhibited a reduction in system COP by 11%. Mota-Babiloni et al. [27] determined the influence of IHX effectiveness variation on system performance at different evaporating temperatures. R513A presented a noticeable reduction in discharge temperature compared to R134a and a cooling capacity and COP benefit when the IHX was used. Velasco et al. [28] concluded that R513A could reduce COP by 24% for a water chiller. Aprea et al. [29] experimentally compared R1234yf, R1234ze(E), a mixture of R1234yf/R134a (90/10 by mass percentage), and the mixture of R1234ze(E)/R134a (90/10 by mass percentage), as alternatives to R134a in a domestic refrigerator. The mixture of

R134a/R1234yf showed 16% energy saving, with a 17% reduction of the LCCP (Life Cycle Climate Performance) compared to R134a. López-Belchí [30] experimentally found that replacing R134a with R513A or R1234yf did not enhance performance and that R134a showed a higher heat transfer coefficient and frictional pressure drop. Thu et al. [31] experimentally investigated an R32/R1234yf/R744 (22/72/6 by mass percentage) mixture as an alternative to R134a for three operation modes: cooling, low temperature, and high-temperature heating mode. The mixture provided the highest system COP at low-temperature heating mode. Sun et al. [32] experimentally showed that R513A presents capacity and COP reduction of 12% for most operating conditions. Al-Sayyab et al. [33] simulated a compound ejector-heat pump system with R450A and R513A for simultaneous cooling and heating. In heating mode, R513A showed system COP reductions by 2% to 5% compared to R134a. Meanwhile, R450A had enhanced system COP in both cooling and heating modes.

Extensive literature review shows that most previous research has focused on studying new synthetic pure and mixture working fluids in R134a refrigeration applications. In addition, these fluids can also be used for heating, particularly at moderate temperature heat pump conditions. Mota-Babiloni et al. [34] considered R1234ze(E) and R515B for moderately high-temperature heat pumps designed for R134a. The experimental results were comparable amongst the test refrigerants, with a 15 and 28% reduction in CO_2-eq emissions for R1234ze(E) and R515B, respectively, and a broader operation range, but significant reduction in heating capacity. R513A received particular attention as a replacement for R134a but can only be considered an interim alternative refrigerant. Due to the GWP value of 631, its usage can be limited in specific applications as directed by the F-Gas Regulation EU 517/2014 phase 3 phase out for refrigerants with GWP above 150 in 2025 [35]. Therefore, the research on the less than 150 low-GWP mixture refrigerant R516A is necessary and meaningful. Al-Sayyab et al. [36] performed a numerical performance comparison for a compound ejector-heat pump system using twelve low global warming refrigerants, including R516A, R1234yf, and R513A. The study improved that R516A and R1234yf have comparable system performance.

R1234yf can form an azeotropic mixture with R134a and R152a (77.5/8.5/14 in mass percentage), provided all of them have comparable boiling points (-29.5 °C, −26.1 °C, and −24.5 °C, respectively). With its lower GWP (1 2 4), R152a considerably reduces the GWP of the blend and tunes the final properties of the mixture. This formulated azeotropic blend has been designated as R516A. According to ASHRAE Standard 34 [37] and ISO-817, R516A is a 2L (mildly flammable refrigerant). It can be considered a long-term solution with a low GWP of 142, which is believed to meet GWP-based phase-down schedules. The thermodynamic properties of R516A can make it a close match to R134a, so it is proposed as a future-proof alternative. There are limited experimental data of R516A to promote its market introduction and deployment and replace R134a (or even R513A).

From an operational and energetic point of view, this work uses experimental data to comprehensively analyse the benefits and limitations of the refrigerants R513A, R516A, and R1234yf, as a compatible replacement for R134a in refrigeration and heat pump systems. To compare these working fluids in the vapour compression system, operational parameters such as compressor consumption power, cooling and heating capacity, and discharge temperatures were measured in two operating modes (heating and cooling). Additionally, the impact of IHX effectiveness variability in cooling mode was studied at different condensing and evaporating temperature levels. Apart from the novelty of presenting R516A experimental results in heating conditions for the first time, the number of experimental tests, detailed description of the vapour compression test bench, and broad range of operating conditions make this paper one of the most extensive assessments of R134a low GWP drop-in assessments.

2. Experimental methodology

2.1. Experimental setup

The schematic diagram is shown in Fig. 1. The system is composed of a fully monitored single-stage system with an IHX vapour compression circuit and two closed-loop with glycol brine and water. The main components of the vapour compression circuit are a scroll compressor, three brazed plate heat exchangers (condenser, evaporator, and internal heat exchanger), and an electronic expansion valve. Additional components are included for a proper system operation: a liquid receiver, filter drier, sight glass, solenoid valve, and manual valves, among other safety devices.

On the other hand, a closed-loop propylene glycol-based circuit (heat load) consists of a variable speed pump, a 100 L storage buffer tank, and three resistances, each with a maximum power of 5.6 kW. One resistance included a PID controller, while others are actuated manually to achieve the appropriate evaporator load. Meanwhile, the other close-loop water-based circuit (heat removal) consists of a variable speed pump, frequency-controlled fan coil, and auxiliary heat pump. The auxiliary heat pump is actuated manually when the air cooler cannot reach the aimed condensing temperature.

To evaluate the IHX influence on system performance, the test rig has two manual valves at the liquid and suction refrigerant pipeline inlet with a bypass pipeline. The suction pipeline valve is gradually opened and closed, regulating the flow of refrigerant circulating through the IHX to reach the targeted effectiveness, which is determined by employing the inlet and outlet temperatures. The test rig includes the number of pressure transducers and K-type thermocouples at the inlet and outlet of each heat pump component. A Coriolis flowmeter was installed for the refrigerant mass flow rate in the liquid line. An electromagnetic flowmeter was used for the secondary glycol and cooling water circuits. A digital wattmeter was adopted for the compressor power consumption. Temperature module NI-9213, transducer module NI-9375, current input module NI-9203 and voltage input module NI-9201 are used for measuring and controlling the system. These modules are connected to a NI chassis cDAQ 9184. Measurements are then represented and stored in a desktop computer and operated by a program developed in the LabVIEW environment. Thermodynamic states of refrigerants are obtained with REFPROP v10.0 [38]. The specifications of the measuring devices are also listed in Table.1.

The test rig includes two independent PID controllers to ensure steady-state tests with minimum deviation in the operational temperatures and higher accuracy in the experimental results. PID controllers designed in LabVIEW compare the target evaporating and condensing temperature with the actual one. Actual evaporating and condensing temperatures are calculated in this software using pressure transducers measurements at the inlet and outlet of the evaporator and condenser and a link with REFPROP.

Firstly, the evaporating temperature PID controls the resistances in the heat load circuit by actuating on the percentage of solid-state relays connected to resistances. A higher percentage of the relays increases the heat load these resistances provide; therefore, glycol and evaporating temperatures are increased. Secondly, the condensing temperature PID is intended for the heat removal circuit and acts over the frequency inverter. It regulates the fan-coil rotational speed so that a higher speed increases heat transfer with the ambient and decreases water and condensing temperatures. PID parameters have been set in situ to obtain an adequate response.

Additionally, a PID in the electronic expansion valve controls the superheating degree at the evaporator outlet, reading evaporator outlet pressure and temperature. The electronic expansion valve PID has integrated the properties of different refrigerants to calculate the superheating degree with these measurements. This device has integrated different operational modes that can be selected to determine the most suitable parameters.

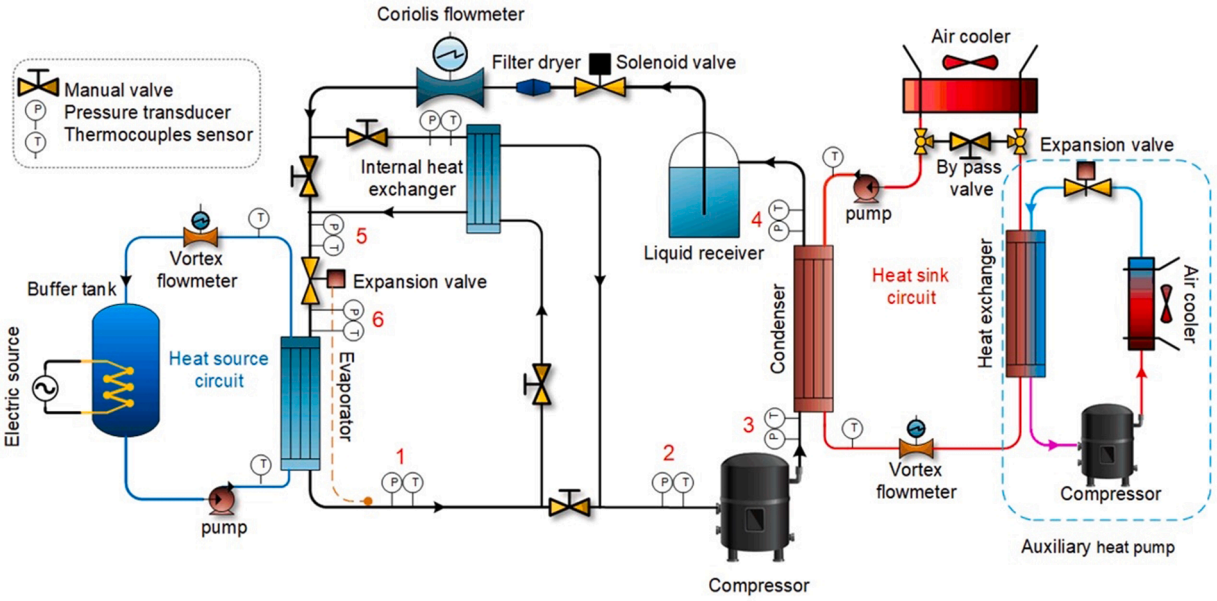

(a)

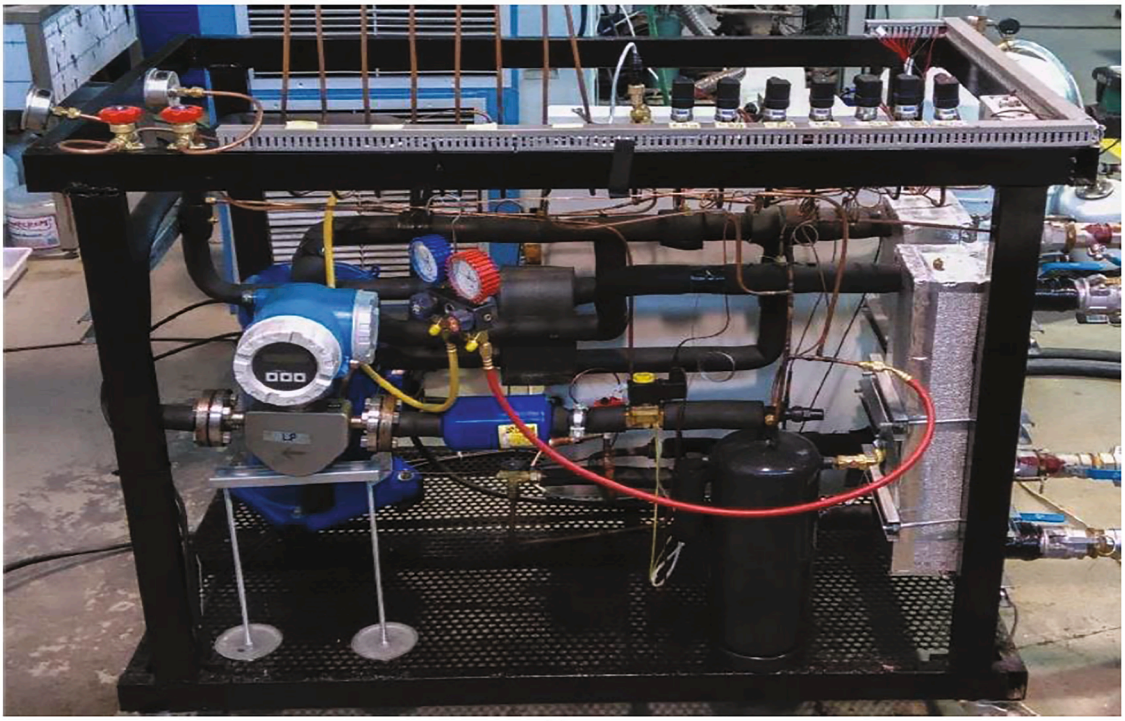

(b)

Fig. 1. Experimental setup: a) schematic diagram and b) picture of the test rig.

Table 1
Specifications of main components and metering devices.

Components	Specifications
Compressor	Danfoss scroll compressor, 17.3 kW at 50 Hz, swept volume of 114.5 cm^3
Condenser	Brazed plate type, 40 plates, heat exchange area of 2.39 m^2
Evaporator	Brazed plate type, 24 plates, heat exchange area of 1.39 m^2
Internal heat exchanger	Brazed plate type, 30 plates, heat exchange area of 0.336 m^2
Water-glycol pump	DAB variable speed pump, 2 to 12 $m^3\ h^{-1}$, −10 °C to 110 °C operating temperature
refrigerant flowmeter	Promass 80 Coriolis flowmeter from Endress, accuracy ± 0.15%, 0 to 100 kg h^{-1}, −40 °C to 125 °C
Water flowmeter	Electromagnetic flow meter, accuracy ± 0.33%, 2 to 30 L min^{-1}
Pressure sensor	Pressure transducer, WIKA S-20, accuracy ± 0.25%, 0 to 40 bar operating range
Temperature sensor	Thermocouple, Type K, accuracy ± 1.5 °C, −40 to 1100 °C operating range
Compressor rotational speed	Frequency inverter, accuracy ± 60 RPM
Power consumption	Digital wattmeter, accuracy ± 1.55% reading

Table 2
Uncertainty analysis results for heating mode and cooling mode.

Mode	Refrigerants	R134a	R1234yf	R516A	R513A
Heating T_e=15 °C T_k=65 °C	Discharge temperature	0.041	0.084	0.03	0.075
	Refrigerant mass flow rate [%]	1.58	2	2.7	2.3
	Heating capacity [%]	1.58	2.02	2.68	2.3
	Compressor power consumption [%]	1.37	1.4	1.4	1.5
	COP_H [%]	2.1	2.5	3.0	2.8
Cooling T_e=−10 °C T_k=40 °C	Refrigerant mass flow rate [%]	2.5	4.8	2.8	2.3
	Cooling capacity [%]	3.8	4.8	2.9	3.3
	Compressor power consumption [%]	1.5	1.4	2.3	1.5
	COP_C [%]	3.1	5.0	3.7	3.9

When the targeted steady-state condition has been reached, the test is monitored and recorded for 30 min with a sampling period of 5 s. Then, the 5 min stable period with the lowest deviation is selected to calculate the average values of the operating condition, which are represented in the graphics included in this paper. The resulting deviation in a test for condensing temperature was 0.05 °C, and for evaporating temperature was 0.07 °C.

Before the experiments, the manual valves were open, and the data acquisition system was switched on. Subsequently, the circulating pumps of the glycol and water loops had started. The test conditions are selected from the platform window interface, target condensing, evaporating temperature, compressor frequency, degree of superheat, and the sampling period of data recording. Then the heat pump was turned on.

Experimental work typically involves indirect measurements of two or more quantities to calculate the desired parameter. When physical quantities cannot be measured with a single direct measurement, a method that transmits the uncertainties of independent variables through an equation is required. Henceforth, uncertainty propagation estimates the uncertainty of the final calculation. This methodology is applied as a built-in procedure in Engineering Equation Solver (EES) [39], Table 2.

2.2. Operating conditions

To evaluate the suitability of the proposed refrigerants as alternatives to R134a in both cooling and heating modes (Table 3, experiments were carried out at three different evaporating temperatures, −15 °C, −10 °C and −5 °C, with the assessment of IHX impact on the overall system performance. Meanwhile, the condensing temperature was set at 32.5 °C and 40 °C.

In addition, to cover different temperature levels observed in waste heat recovery applications (for example, data centre, PV/T, or industrial processes), the heating mode involves different evaporating temperatures, ranging from 7.5 °C to 22.5 °C, in 7.5 °C increments. Meanwhile, the condensing temperature ranged from 55 °C to 75 °C, in 5 °C increments (recommended range for district heating). The electronic expansion valve PID controller maintains the superheating degree in cooling and heating modes at 11 K and 5 K, recommended by the compressor manufacturer datasheet for these conditions [40]. Moreover, all tests are performed with a fixed compressor speed of 2030 RPM, set by the compressor frequency inverter. The compressor manufacturer's maximum allowable suction and discharge temperatures should be less than 50 and 150 °C, respectively.

During the experimental campaign, each steady-state system was recorded for 30 min. The sampling interval was 5 s. The most consistent 5 min range has been selected to obtain the average values of the targeted operating condition. The thermodynamic properties of refrigerants are determined using REFPROP v10.0 software [38].

In this work, previous experimental results of Mota-Babiloni et al. [27,34] are included to be compared with the new R1234yf, R516A (cooling and heating modes), and R513A (heating mode) test results.

2.3. Low global warming refrigerants

In the current study, three low GWP refrigerants, R513A, R516A, and R1234yf, are evaluated for their suitability as a drop-in replacement of R134a, Table 4. R1234yf is a pure HFO with excellent thermal and chemical stability, low toxicity, zero ozone depletion potential, low GWP, mildly flammability, and low toxicity (A2L group). It is highly compatible with most materials used with R134a. This fluid is also a component of R513A and R516A mixtures. R513A consists of R1234yf/R134a (56/44 by mass percentage) and R516A of R1234yf/R152a/R134a (77.5/14/8.5 by mass percentage). Both are azeotropic blends with no temperature glide. R513A is non-flammable, but the higher composition of flammable refrigerants makes R516A mildly flammable (A2L). However, R516A has a GWP (100-year time horizon) below 150, and R513A has a moderate value (631).

The closest molecular weight to R134a is R516A, while R513A is between the HFC and R1234yf. The critical temperature of alternatives is below R134a, so they are not appropriate for cooling at extreme ambient conditions or high-temperature heat conditions. The critical temperature of the mixtures is up to 6.3 K lower than that of R134a. Vapour densities of the lower GWP refrigerants are higher than R134a but exhibit lower latent heat of vaporisation. The lower normal boiling point (NBP) is suitable for medium-to-low refrigeration applications.

Table 3
Experimental boundary conditions.

Parameters	Cooling	Heating
Condensing temperature	32.5 °C and 40 °C	55 °C to 75 °C
Evaporating temperature	−15 °C to −5 °C	7.5 °C to 22.5 °C
Glycol temperature difference across the evaporator	5 °C	12 °C
Condenser's cooling water temperature difference	6 °C	20 °C
Compressor rotational speed	2030 RPM	2030 RPM
Compressor displacement volume	114.5 cm^3	114.5 cm^3

Table 4
Thermophysical properties of the tested refrigerants [37,39].

Refrigerant	Molecular weight (g mol^{-1})	T_{crit} (°C)	P_{crit} (bar)	ρ_{vapor} [a] kg m^{-3}	ρ_{liquid} [a] kg m^{-3}	h_{fg} [a] kJ kg^{-1}	NBP (°C)	ODP	GWP_{100}	Safety class ASHRAE
R134a	102.03	101.0	40.59	5.258	1377	217.0	−26.09	0	1430	A1
R513A	108.40	94.91	36.47	5.696	1314	194.8	−29.52	0	631	A1
R516A	102.58	97.30	36.45	5.929	1321	188.5	−29.40	0	142	A2L
R1234yf	114.0	94.70	33.82	5.963	1263	180.3	−29.49	0	4	A2L

[a]At a pressure of 1.01325 bar.

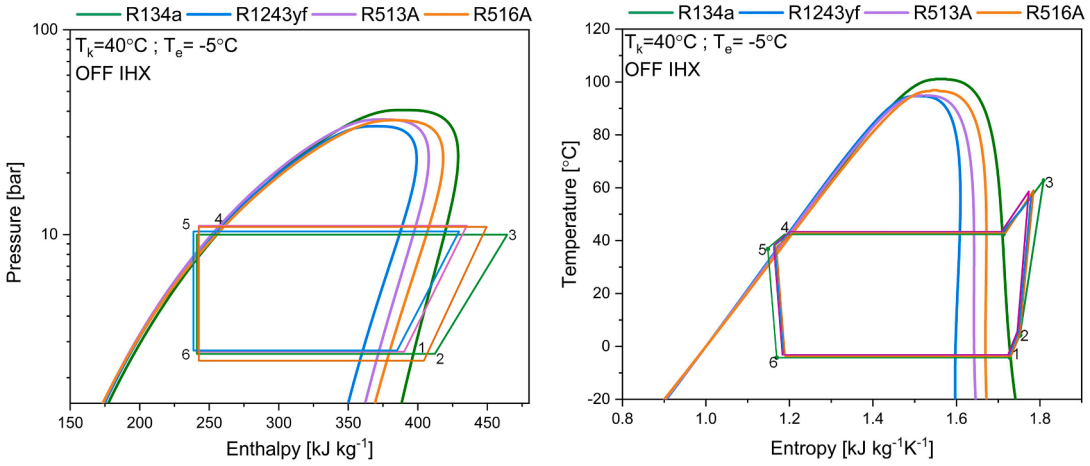

Fig. 2. P-h and T-s diagram cycle of tested refrigerants.

Fig. 2 depicts the pressure-enthalpy and the temperature-entropy cycle diagrams of the refrigerants included in this work. It evidences the differences in the critical point and latent heat of vaporisation.

2.4. Equations

The compressor volumetric and isentropic efficiencies are calculated as follows, Eq. (1) and (2).

$$\eta_v = \frac{\dot{m}}{\left(\frac{RPM}{60}\right)\frac{V_{DS}}{v_S}} \tag{1}$$

$$\eta_{is} = \frac{\dot{m}\Delta h_{is,c}}{\dot{W}_c} \tag{2}$$

Heating capacity can be obtained from Eq. (3) and (4), multiplying the refrigerant specific enthalpy difference across the condenser (heating effect) by the refrigerant mass flow rate.

$$\dot{Q}_k = \dot{m}\ q_k \tag{3}$$

$$q_k = \left(h_{k,in} - h_{k,out}\right) \tag{4}$$

Similarly, the cooling capacity can be obtained from Eq. (5) and (6), multiplying the refrigerant specific enthalpy difference across the evaporator (refrigerating effect) by the refrigerant mass flow rate.

$$\dot{Q}_e = \dot{m}\ q_e \tag{5}$$

$$q_e = \left(h_{e,out} - h_{e,in}\right) \tag{6}$$

To have an IHX with a wide range of effectiveness, the experimental set consists of a high effectiveness IHX and a bypass. In this way, the heat exchanger effectiveness can be changed to the equivalent IHX measuring at the inlet and the set outlet, as shown in Fig. 3.

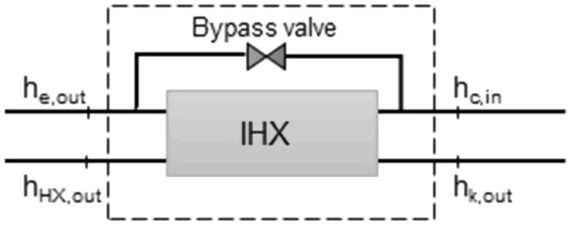

Fig. 3. IHX effectiveness evaluation.

The internal heat exchanger effectiveness can be evaluated by Eq. (7).

$$\varepsilon_{IHX} = \frac{h_{c,in} - h_{e,out}}{h_{k,out} - h_{e,out}} \tag{7}$$

The system coefficient of performance in cooling (COP_C) and heating (COP_H) mode results from Eq. (8) and Eq. (9), respectively

$$COP_C = \frac{\dot{Q}_e}{\dot{W}_c} \tag{8}$$

$$COP_H = \frac{\dot{Q}_k}{\dot{W}_c} \tag{9}$$

3. Results and discussion

3.1. Heating mode

Heating mode aims to use low-temperature heat coming from data centres, PV/T systems, industrial processes, or even outside air, and revalorise the high-temperature used for different purposes such as district heating in urban or industrial environments. Therefore, this

section shows the influence of condensing temperature of 55 °C to 75 °C on system performance at evaporating temperatures of 7.5 °C, 15 °C, and 22.5 °C. At the same time, the main operating and energetic parameters are represented in the Y-axis versus the condensing temperature in the X-axis. The parameters analysed are refrigerant mass flow rate, volumetric efficiency, pressure ratio, compressor consumption power, discharge temperature, heating capacity and COP.

Fig. 4 contains the experimental measurements of refrigerant mass flow rate. Both compressor pressure ratio and refrigerant suction density directly influence this parameter. The increasing condensing temperature at constant evaporation temperatures reduces the mass flow rate due to the pressure ratio increase, leading to lower volumetric efficiency values. On the other hand, the evaporator temperature increase positively affects refrigerant mass flow rate at constant condensing temperature. This effect is caused by increased refrigerant density and volumetric efficiency (Fig. 5) due to a pressure ratio decrease (Fig. 6).

Compared to R134a, in the tested conditions, both alternative refrigerants R1234yf and R513A showed much higher average refrigerant mass flow rates (around 23% and 17%, respectively). Meanwhile,

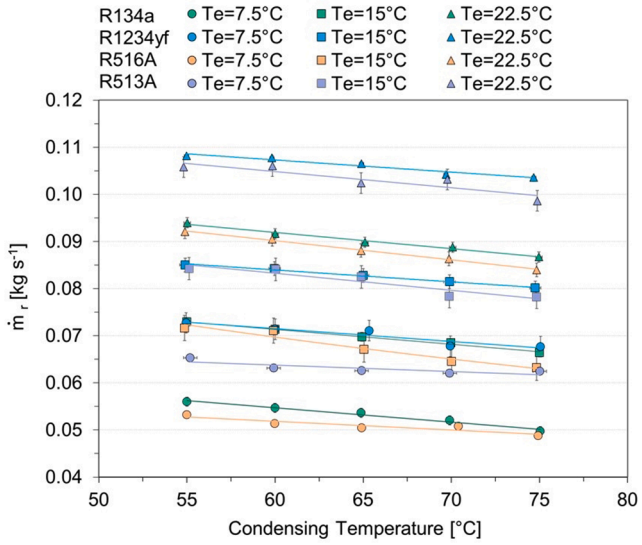

Fig. 4. Refrigerant mass flow rate versus condensing temperature.

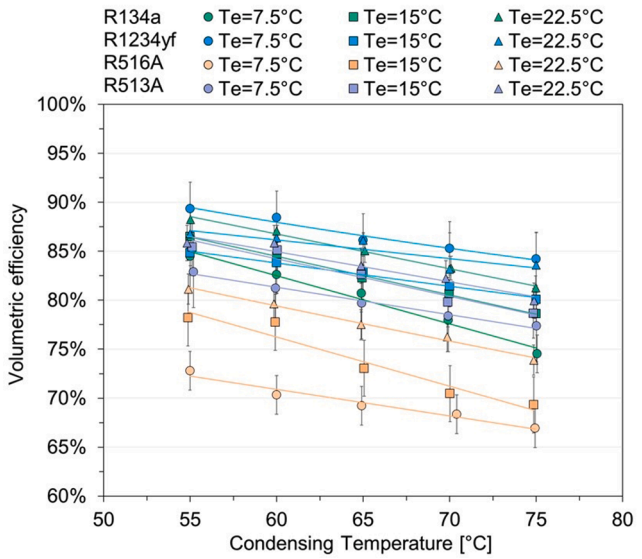

Fig. 5. Compressor volumetric efficiency versus condensing temperatures.

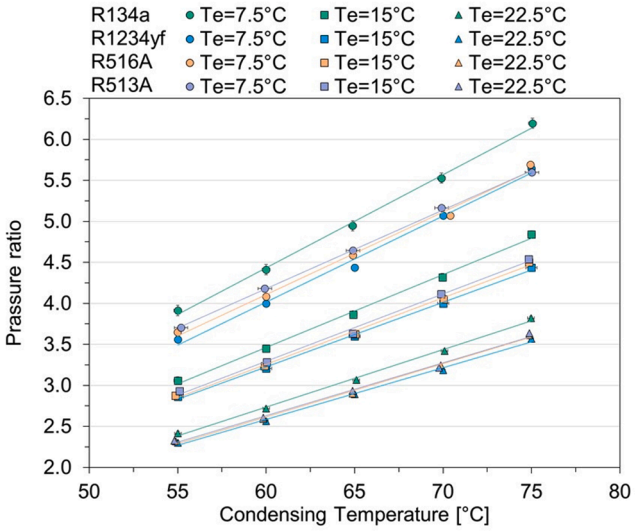

Fig. 6. Compressor pressure ratio at different condensing temperatures.

R516A shows the closest to R134a, about 3%. On the other hand, both R513A and R1234yf result in comparable mass flow rates at higher evaporating temperatures. R516A shows closer values to R134a at all testing conditions. However, R516A ends with the lowest average volumetric efficiency, making larger compressor displacement necessary to match R134a heating capacity. Overall, R1234yf shows the highest volumetric efficiency. Finally, the compressor pressure ratio of alternative refrigerants is close to that of R134a at higher evaporating temperatures.

One of the most critical parameters in the heating mode is the condenser heating capacity. Attending to what can be seen in Fig. 7, the condensing temperature negatively influences the heating capacity at a constant evaporating temperature. The previously analysed mass flow rate reduction is combined with a heating effect reduction, observed in Fig. 8.a. In comparison, R513A has the highest heating capacity delivered overall testing conditions with a 3% average heating capacity enhancement. Meanwhile, R516A shows the lowest at the highest evaporating temperature. It means that R516A requires less condensing area than tested refrigerant. The increasing evaporating temperature enhances system heating capacity at constant condensing temperature

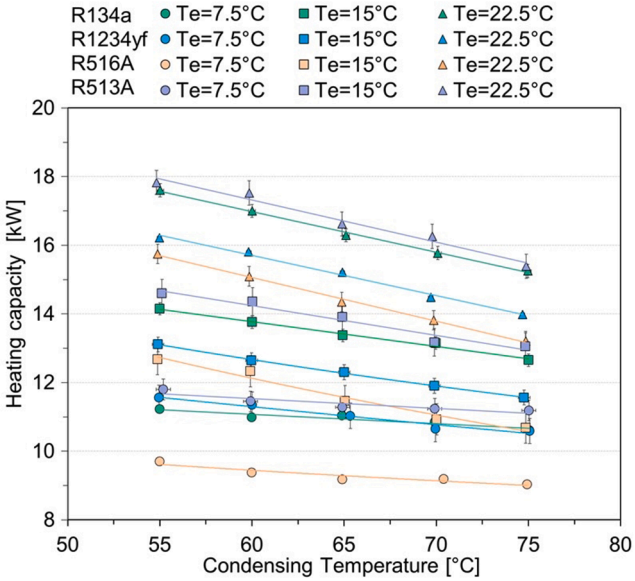

Fig. 7. Heating capacity versus condensing temperature

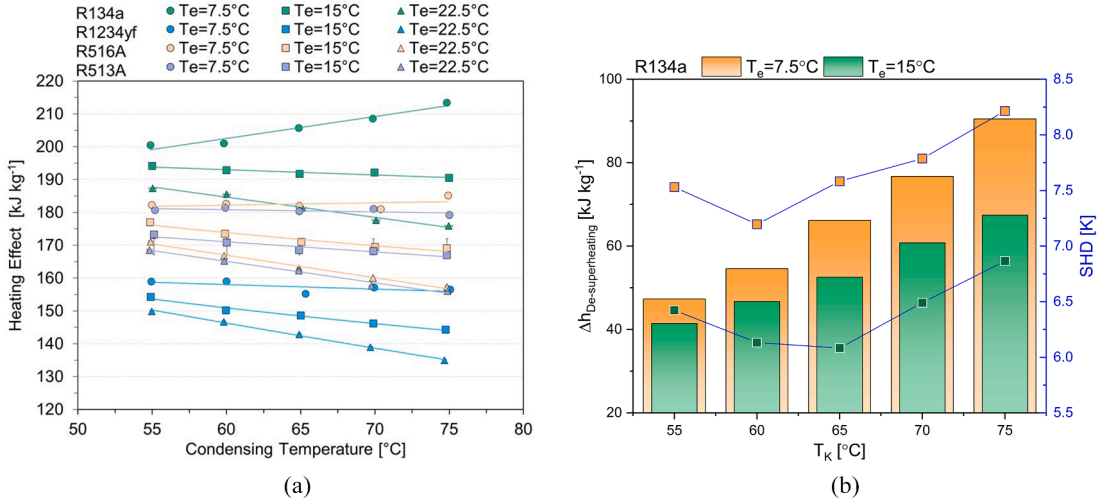

Fig. 8. a. Heating effect versus condensing temperature. b. Superheating degree versus condensing temperature.

due to the pressure ratio decrement (Fig. 6) as the refrigerant mass flow rate increases (Fig. 4). R1234yf matches R134a heating capacity at a low evaporating temperature, while R513A provides comparable heating capacity at a high condensing temperature.

The heating effect is proportional to the condensing temperature at the evaporating temperature of 7.5 °C, as opposed to other evaporating conditions, Fig. 8.a. This is caused by a higher superheating degree, which positively affects the desuperheating process [41], as well as the heating effect, Fig. 8.b.

Fig. 9 illustrates the compressor consumption power from direct experimental measurements. It is evidenced that for all tested refrigerants, the consumption power increases with the condenser temperature increasing. Meanwhile, the increase in evaporating temperature slightly reduces compressor consumption power due to pressure ratio reduction with refrigerant mass flow rate increasing (one offset the other). Compared with R134a, the alternative refrigerant R513A has the highest consumption power. Meanwhile, R516A and R1234yf show the lowest values.

There are many potential causes of compressor lifetime reduction; the most important is excessive discharge temperature. From experimental measurements, Fig. 10 shows that, at constant evaporating temperature, an increase in condensing temperature led to a higher discharge temperature. This point reflects all heat absorbed by the refrigerant during the evaporation, superheating and compression processes (Fig. 9).

In comparison, the alternatives showed lower discharge temperatures at all tested conditions. Among the lower GWP refrigerants, R1234yf has the lowest discharge temperature (on average, a reduction

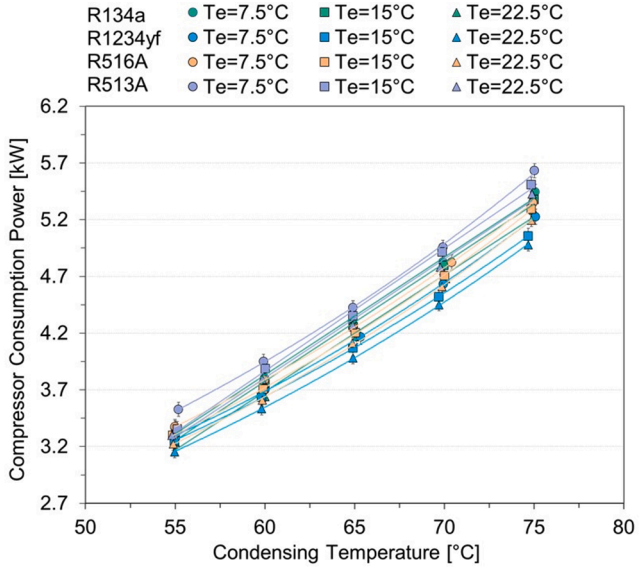

Fig. 9. Consumption power versus condensing temperature.

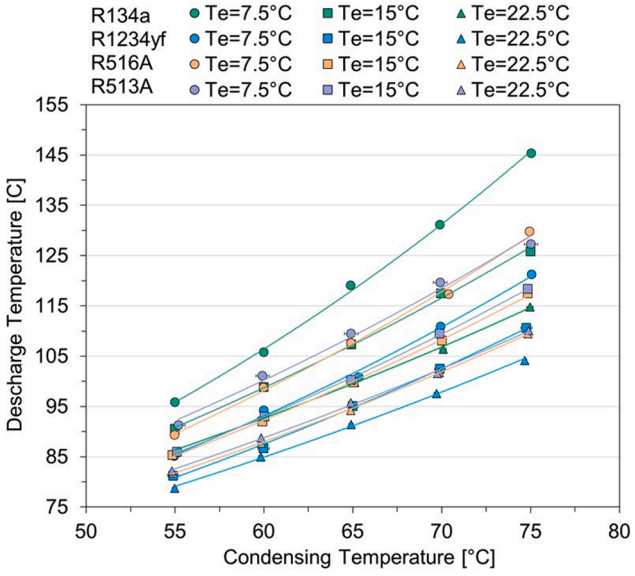

Fig. 10. Discharge temperature versus condensing temperature.

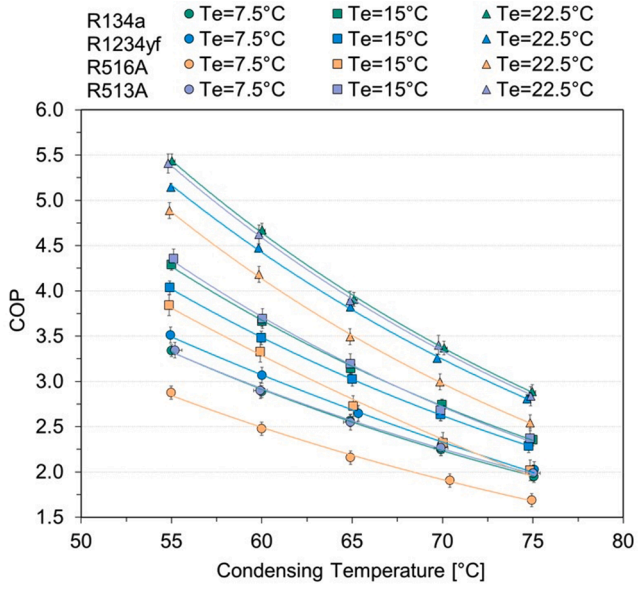

Fig. 11. Heating COP versus condensing temperature.

of 11 °C). Therefore, operation with this fluid would offer prolonged operation of the compressor lubricating oil and increased compressor lifespan.

Fig. 11 exhibits the COP as the indicator of refrigerant performance. At constant evaporating temperatures, increasing condensing temperature decreases COP for all tested refrigerants due to compressor consumption power increase, representing the factor that takes a dominant role associated with heating capacity decreasing. On the other hand, the evaporating temperature improves COP at constant condensing temperature, owing to a consumption power decrease (Fig. 9) associated with a heating capacity increase (Fig. 7).

To summarise and represent relative deviations in COP (Fig. 12), R516A shows the lowest system performance relative to R134a at all tested conditions, with an average reduction of 4% to 12%. Noteworthy, in the same context, at the evaporating temperature of 7.5 °C, R1234yf shows the highest system performance at moderate condensing temperatures (55 °C to 65 °C) with a 4% average system COP enhancement. Meanwhile, R513A COP is comparable to R134a at all tested conditions. It can be adopted as an appropriate alternative refrigerant to R134a in the heating mode.

3.2. Cooling mode

Cooling mode targets refrigeration at medium temperatures, observed in industrial or commercial processes. Selected condensing temperatures can be typically observed in regions not reaching extreme (cold or warm) conditions. Consequently, figures included in this section shows experimental results at different evaporating temperatures (-15 °C, −10 °C and −5 °C) and two condensing temperatures (32.5 °C and 40 °C). Again, the experimental parameters shown are refrigerant mass flow rate, pressure ratio, compressor consumption power, discharge temperature, cooling capacity and COP. This section's interesting and novel fact is that the influence of the IHX effectiveness on system performance is studied.

As in the previous section, the first parameter to be analysed is the refrigerant mass flow rate (Fig. 13). Similar thermodynamic analysis can be applied with the addition of Fig. 13.b. Increasing the IHX effectiveness reduces the refrigerant mass flow rate delivered due to higher superheating and, hence, lower compressor suction density. In contrast, when comparing 40% IHX effectiveness actuation with the off case, R513A exhibits the most significant mass flow rate reduction (7.7% to 9.6%) at defined evaporating temperature, followed by R1234yf (3% to 9%); meanwhile, R516A shows the lowest reduction (2.3% to 3.7%). In comparison to R134a, all tested low GWP refrigerants have a higher mass flow rate, with R1234yf exhibiting the highest increase in mass flow rate ranging from 33% to 61%.

A critical factor in the cooling mode is the cooling capacity, which depends on both refrigerant mass flow rate and refrigerating effect. From Fig. 14, at a given evaporating temperature, the IHX actuation significantly enhances the refrigerating effect due to refrigerant mass flowrate reduction (Fig. 13) with constant glycol heat source capacity. On the other hand, for the OFF case, the higher the evaporation temperature, the higher the refrigerating effect because of the slope of the

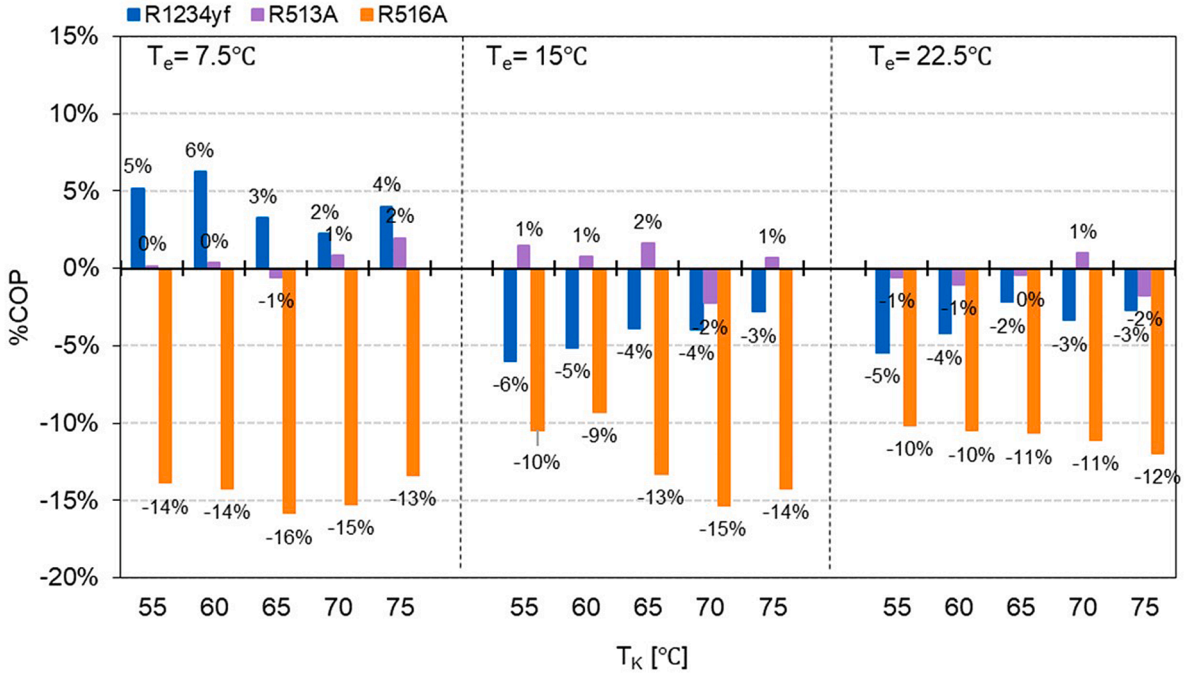

Fig. 12. System COP increase at different evaporation temperatures.

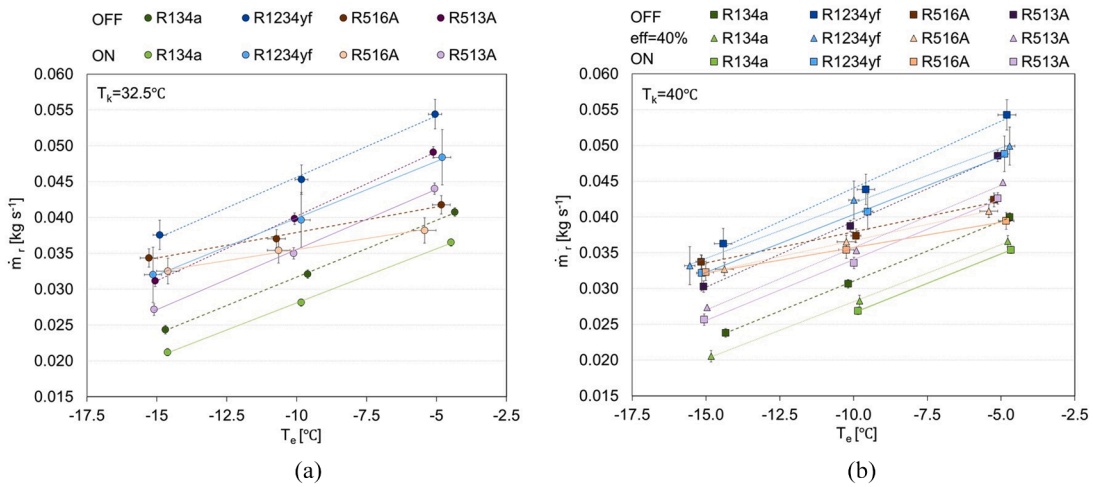

Fig. 13. Refrigerant mass flow rate at different evaporating temperatures with internal heat exchanger actuation for a) condensing temperature of 32.5 °C and b) condensing temperature of 40 °C.

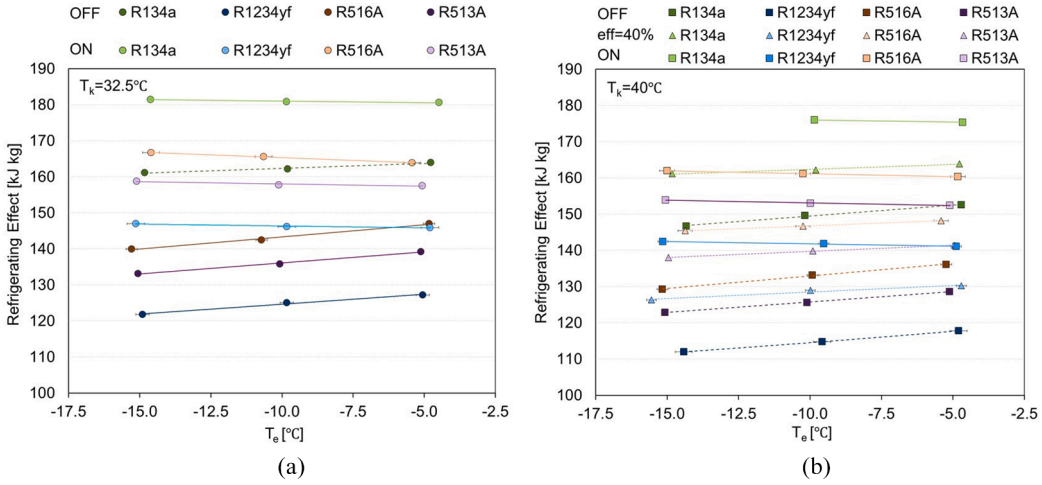

Fig. 14. Refrigerant effect at different evaporating temperatures with internal heat exchanger actuation for a) condensing temperature of 32.5 °C and b) condensing temperature of 40 °C.

saturated vapour line. Then, it should be considered that the evaporator superheating degree and the total subcooling degree are comparable. When the IHX is activated (ON case), this difference is compensated by the additional subcooling degree introduced by the IHX, which is higher at lower evaporating temperatures. This is reflected in the evaporator refrigerating effect.

In the same contexts, at constant condensing temperature, the higher evaporating temperature, the higher refrigerating effect, resulting from a slight superheating degree increase. R516A displays the highest refrigerating effect compared with all tested refrigerants, whereas R1234yf has the lowest.

Moreover, when comparing 40% IHX effectiveness actuation with the off case at defined evaporating temperature, R1234yf exhibits the most significant refrigerating effect enhancement (10.6% to 12.8%); meanwhile, R516A shows the lowest (8.8% to 12.5%). In contrast, in the case of full IHX actuated, it is seen in Fig. 14.b that the IHX positively affects refrigerating effect by increasing the degree of subcooling. The highest benefit is observed with R1234yf, from 20% to 27%.

Fig. 15 focuses on cooling capacity evolution. R1234yf shows an 11% to 22% cooling capacity increase compared to R134a. The IHX effectiveness increasing has a final positive influence on the cooling capacity (Fig. 15.b), owing to a dominant refrigerating effect increase. In the case of 40% IHX effectiveness actuating compared with the previous IHX off case, R516A exhibits the highest cooling capacity improvement (4.8% to 9.1%); on the other hand, R513A exhibits the lowest increase (1% to 2%). R516A shows the highest cooling capacity at a low evaporating temperature (-15 °C and −10 °C), indicating that R516A is suitable for low-temperature applications.

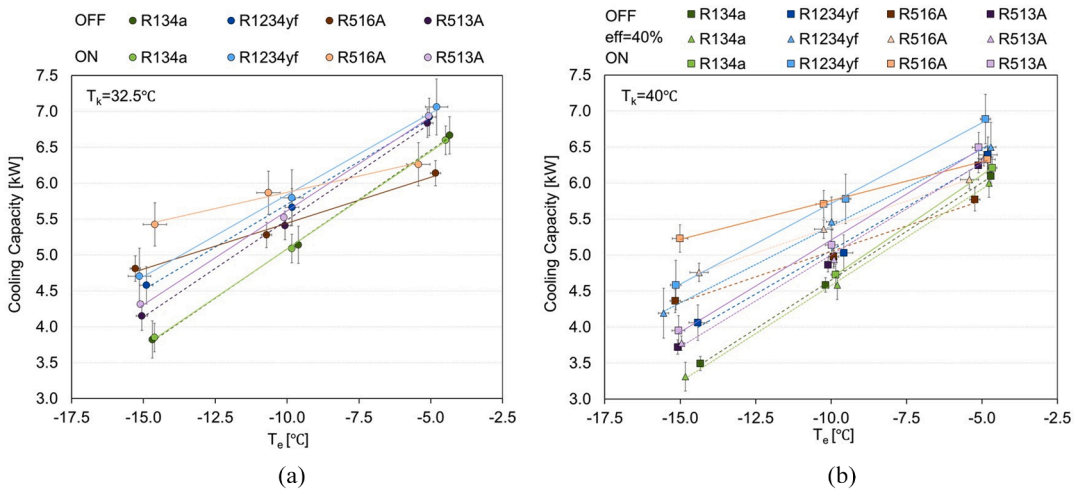

Fig. 15. Refrigerant capacity at different evaporating temperatures with internal heat exchanger actuation for a) condensing temperature of 32.5 °C, and b) condensing temperature of 40 °C.

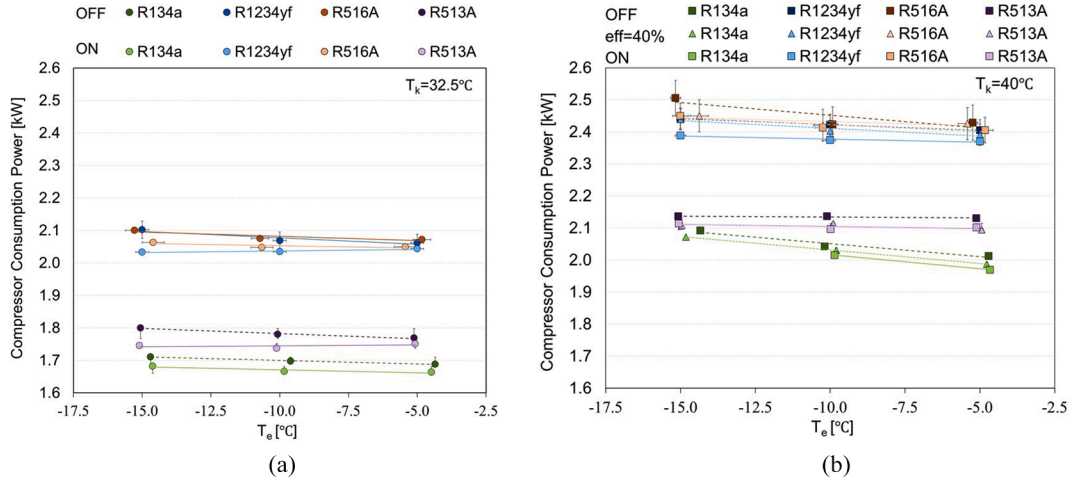

Fig. 16. Compressor power at different evaporating temperatures with internal heat exchanger actuation for a) condensing temperature of 32.5 °C and b) condensing temperature of 40 °C.

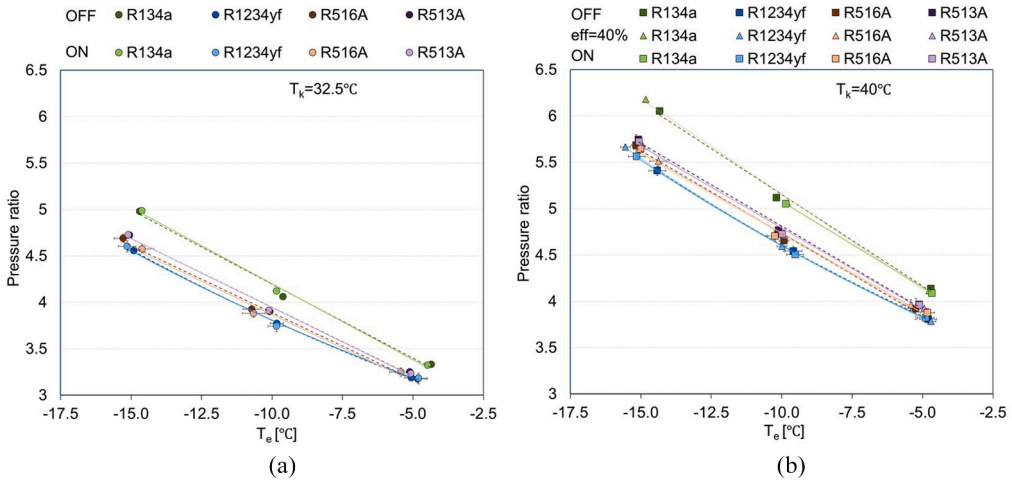

Fig. 17. Compressor pressure ratio at different evaporating temperatures with internal heat exchanger actuation for a) condensing temperature of 32.5 °C, and b) condensing temperature of 40 °C.

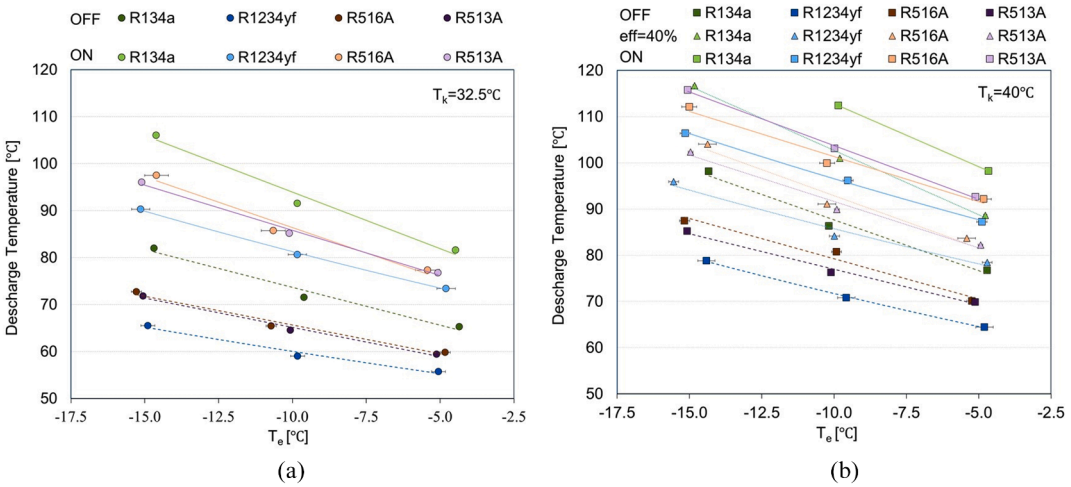

Fig. 18. Discharge temperature at different evaporating temperatures with internal heat exchanger actuation for a) condensing temperature of 32.5 °C, and b) condensing temperature of 40 °C.

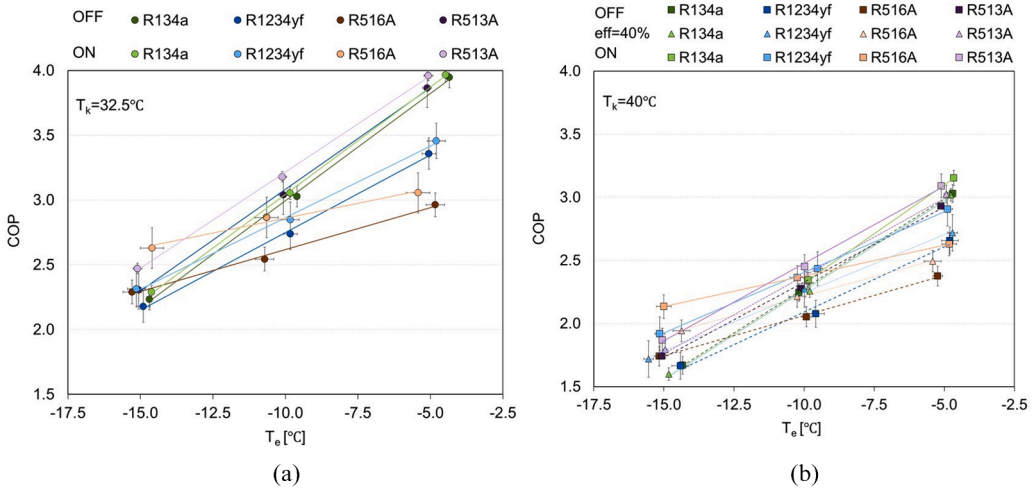

Fig. 19. Coefficient of performance at different evaporating temperatures with internal heat exchanger actuation for a) condensing temperature of 32.5 °C and b) condensing temperature of 40 °C.

The compressor consumption power is another parameter that was directly measured. This time, R516A shows the highest values. On the other hand, the IHX effectiveness increase reduces compressor consumption power (Fig. 16.b), given the reduction in refrigerant mass flow rate (Fig. 13), with unremarkable influence on compressor pressure ratio (Fig. 17).

Fig. 18 shows that, at constant condensing temperature, an increase in evaporating temperature lowers the discharge temperature values, owing to the increase in the refrigerant mass flow rate (Fig. 13). Again, compared to R134a, the tested low GWP refrigerants ended with lower discharge temperature at all tested conditions. Similar to the heating mode, R1234yf has the lowest discharge temperature (on average, a reduction of 13.5 °C). In the same context, IHX actuation increases discharge temperature for all tested refrigerants (Fig. 18.b).

As previously discussed, an increase in evaporating temperature positively influences the cooling capacity (Fig. 15) by increasing the refrigerant mass flow rate and slightly reducing the consumption power. (Fig. 16). As a result, the increasing evaporative temperature has enhanced system COP for all tested refrigerants (Fig. 19). Higher condensing temperatures reduce system COP at constant evaporating temperature due to the compressor consumption power increase (pressure ratio) (Fig. 17) with a degree of subcooling decrement. On the other hand, the IHX improves COP (owing to consumption power reduction and cooling capacity increase). Compared with an IHX off case, when 40% IHX effectiveness is actuated at a defined evaporating temperature, R516A has the highest COP enhancement (4.9% to 11.6%), while R513A shows the lowest (2.6% to 3.3%) Fig. 19.b. Finally, R513A presented the highest system COP compared to all tested refrigerants with an average increase of 2%. Meanwhile, R516A shows the highest performance at all condensing temperatures and low evaporative temperatures. At the same time, it shows the lowest COP at the highest evaporative temperature (Fig. 19).

Fig. 20 summarises the relative values compared to R134a. At a condensing temperature of 32.5 °C and an evaporating temperature of −15 °C, refrigerant R516A presents the highest system COP enhancement by 15% with IHX compared to R134a. Finally, R513A delivers

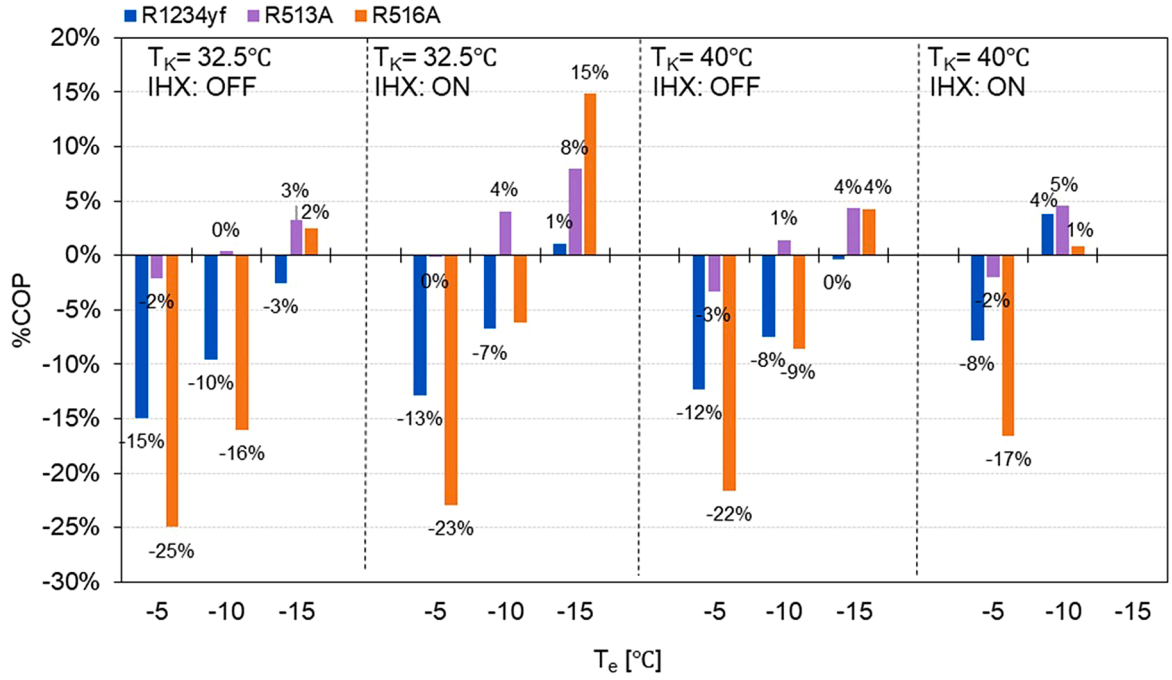

Fig. 20. Relative COP compared to R134a.

comparable system performance with an enhancement of up to 8%. The highest enhancement is recorded when the condensing temperature is 32.5 °C, and the evaporating temperature is −15 °C with the utilisation of IHX. It should be mentioned that the system cannot reach conditions of 40 °C condensing temperature and −15 °C evaporating temperature associated with IHX actuation due to the higher degree of superheat (out of compressor manufacturer recommended range). The compressor cannot operate with a discharge temperature above 150 °C or a suction temperature higher than 50 °C.

Fig. 21 shows the IHX effectiveness for full actuation (ON case) at a condensing temperature of 32.5 °C and different evaporating temperatures. Refrigerant R134a presents the highest IHX effectiveness for all evaporating temperatures compared to tested refrigerants. Finally, R516A shows the highest IHX effectiveness compared to the tested low GWP refrigerants at the evaporating temperature of −15 °C.

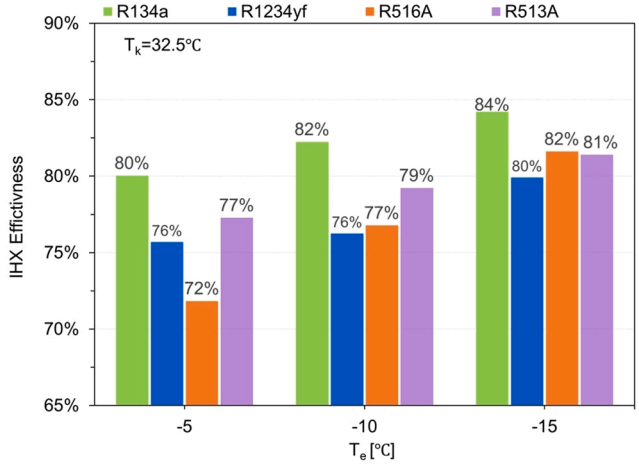

Fig. 21. IHX effectiveness for ON case at different evaporating temperatures.

3.3. Carbon footprint comparison

The global warming impact of HVAC equipment can be measured in carbon dioxide equivalent emissions (CO_2-eq) by a metric named Total Equivalent Warming Impact (TEWI). It is based on the greenhouse gas emissions during the unit's operation, including electricity consumption and the accidental losses of refrigerant. Also, it accounts for the refrigerant losses when recovering refrigerant.

Henceforth, TEWI considers both direct and indirect emissions, calculated as shown in Eq. (10) [42].

$$TEWI = GWP\ m\ L\ n + GWP\ m\ (1)-\alpha + n\ E\ \beta \quad (10)$$

The carbon footprint analysis considers two operating conditions, one for the heating mode (T_k = 65 °C, T_e = 7.5 °C), in which all refrigerants show comparable heating capacity and only R516A; and another for the cooling mode (T_k = 40 °C, T_e = −10 °C), in which all refrigerants have equivalent cooling capacity at this condition. To prevent cooling and heating capacity inequivalence in TEWI calculations, TEWI results are normalised to the cooling and heating capacity of the respective refrigerant ($TEWI_N$).

Fig. 22 presents the $TEWI_N$ relative reduction using low GWP alternatives to R134a. Different carbon emission factors and refrigerant leak ratios are analysed under different scenarios. The heat pump lifetime (n) is considered 15 years; the operating period for heating and cooling modes are 4 and 6 months, respectively. R1234yf presents the highest $TEWI_N$ reduction in heating modes ranging from 11% to 58%. R516A shows a lower $TEWI_N$ reduction than R513A in the heating mode, whereas, in cooling mode, R513A and R516A show comparable $TEWI_N$ reduction, from 40% to 86%, and R1234yf shows the highest reduction, from 45% to 93%.

4. Conclusions

Low GWP refrigerants R1234yf, R513A, R516A were compared to R134a in a test rig at a wide range of operating conditions. In cooling

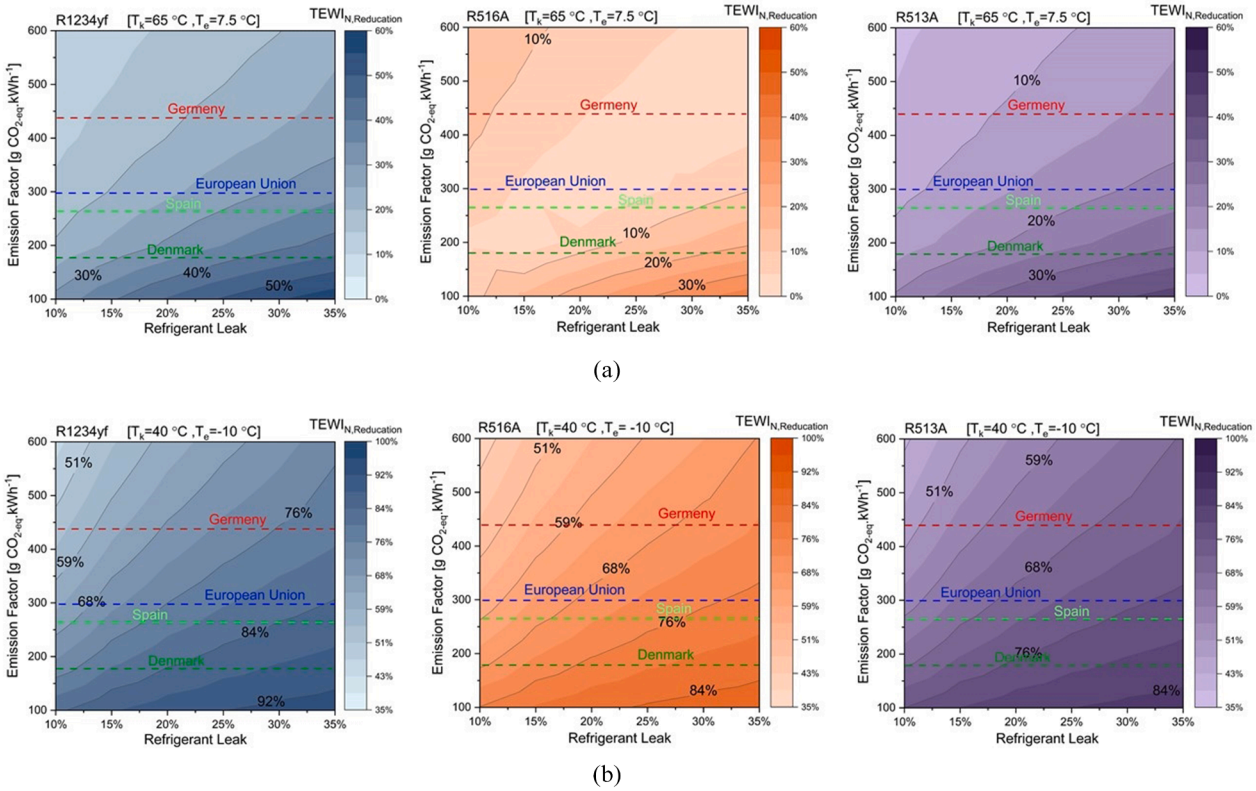

Fig. 22. $TEWI_N$ reduction using R134a drop-in low GWP alternatives for a) heating conditions of $T_k = 65\ °C$; $T_e = 7.5\ °C$. and b) cooling conditions of $T_k = 40\ °C$, $T_e = -10\ °C$.

mode, the evaporating temperature was −5 °C, −10 °C, and −15 °C, and the condensing temperature was 32.5 °C and 40 °C, which included a study of the IHX effect. On the other hand, in heating mode, the evaporating temperature was 7.5 °C, 15 °C and 22.5 °C, evaluated at five condensing temperatures (55 °C to 75 °C, increments of 5 °C).

The experimental conclusion can be drawn as follows:

1. The novel mixture R516A exhibits the closest refrigerant mass flow rate to R134a in heating mode, with a deviation of 3%. Meanwhile, R1234yf and R513A have significantly higher refrigerant mass flow rates than R134a, 23% and 17%, respectively. R1234yf presented the highest mass flow rate in cooling mode, 33% to 61% higher than R134a.
2. R513A has the highest heating capacity, with a 3% average increase compared to R134a. R516A results in the lowest heating capacity values. Besides, the R1234yf cooling capacity is 11% to 22% higher than R134a. As in the heating mode, R516A shows the lowest cooling capacity results.
3. R513A presents the highest consumption power, followed by R516A. However, these results should be complemented by the analysis of the COP. Thus, R513A results in the highest system COP in cooling mode, with a 4% to 5% increase with IHX. R516A shows the highest COP at the lowest evaporating temperature, −15 °C, with a system COP increase ranging from 2% to 15%. R516A presents the lowest COP in heating mode, with a 10% to 15% reduction compared to R134a.
4. At different refrigerant leakage ratios, for the Spanish electric mix (265.4 gCO_2-eq kWh^{-1}), R1234yf presents the highest normalised TEWI reduction in both modes, 58% heating and 93% (cooling). R516A shows a lower decrease than R513A in the heating mode.
5. Finally, the refrigerant R513A shows comparable performance to R134a at all tested conditions. Moreover, this work confirms that R516A is a potential alternative for low evaporating temperatures in refrigeration systems, but it requires modifications to match R134a cooling and heating capacity.

Declaration of Competing Interest

The authors declare that they have no known competing financial interests or personal relationships that could have appeared to influence the work reported in this paper.

Acknowledgements

Ali Khalid Shaker Al-Sayyab gratefully acknowledges the Southern Technical University in Iraq for the financial support. Adrián Mota-Babiloni acknowledges “Juan de la Cierva-Incorporación 2019” contract (IJC2019-038997-I), funded by Spanish State Research Agency (MCIN/AEI/10.13039/501100011033).

References

[1] ECMWF C. Copernicus: 2020 warmest year on record for Europe; globally, 2020 ties with 2016 for warmest year recorded, 2020.
[2] severe-weather 2021. https://www.severe-weather.eu/europe-weather (accessed 10 August 2021).
[3] IEA. The Future of Cooling: Opportunities for energy-efficient air conditioning. Futur Cool Oppor Energy-Efficient Air Cond 2018:92.
[4] United Nations Environment Programme (UNEP). Handbook for the Montreal Protocol on Substances that Delete the Ozone Layer Thirteenth edition (2019), ISBN: 978-9966-076-59-5. 2019.
[5] Paardekooper, S, Lund, RS, Mathiesen, BV, Chang, M, Petersen, UR, Grundahl, L, David, A, Dahlbæk, J, Kapetanakis, IA, Lund, H, Bertelsen, N, Hansen, K, Drysdale, DW & Persson U 2018. Heat Roadmap Europe 4 : Quantifying the Impact of Low-Carbon Heating and Cooling Roadmaps. 2018.
[6] EUROPEAN COMMISSION. Analysis of options beyond 20% GHG emission reductions: Member State results. Brussels: 2012.
[7] Epa US. Phasedown of hydrofluorocarbons: Establishing the allowance allocation and trading program under the American innovation and manufacturing act. Fed Regist 2021;86:27150–223.

[8] Mota-Babiloni A, Makhnatch P, Khodabandeh R. Recent investigations in HFCs substitution with lower GWP synthetic alternatives: Focus on energetic performance and environmental impact. Int J Refrig 2017;82:288–301. https://doi.org/10.1016/j.ijrefrig.2017.06.026.
[9] EEA. Fluorinated greenhouse gases 2020. 2020.
[10] Honeywell. Honeywell. 2010 n.d. http://www51.honeywell.com/honeywell/news-events/press-releases-details/10_0520_Honeywell_Dupont.html.
[11] Sethi A, Vera Becerra E, Yana MS. Low GWP R134a replacements for small refrigeration (plug-in) applications. Int J Refrig 2016;66:64–72. https://doi.org/10.1016/j.ijrefrig.2016.02.005.
[12] de Paula CH, Duarte WM, Rocha TTM, de Oliveira RN, Mendes R de P, Maia AAT. Thermo-economic and environmental analysis of a small capacity vapor compression refrigeration system using R290, R1234yf, and R600a. Int J Refrig 2020;118:250–60. https://doi.org/10.1016/j.ijrefrig.2020.07.003.
[13] de Paula CH, Duarte WM, Rocha TTM, de Oliveira RN, Maia AAT. Optimal design and environmental, energy and exergy analysis of a vapor compression refrigeration system using R290, R1234yf, and R744 as alternatives to replace R134a. Int J Refrig 2020;113:10–20. https://doi.org/10.1016/j.ijrefrig.2020.01.012.
[14] Janković Z, Sieres Atienza J, Martínez Suárez JA. Thermodynamic and heat transfer analyses for R1234yf and R1234ze(E) as drop-in replacements for R134a in a small power refrigerating system. Appl Therm Eng 2015;80:42–54. https://doi.org/10.1016/j.applthermaleng.2015.01.041.
[15] Sieres J, Santos JM. Experimental analysis of R1234yf as a drop-in replacement for R134a in a small power refrigerating system. Int J Refrig 2018;91:230–8. https://doi.org/10.1016/j.ijrefrig.2018.05.019.
[16] Li Z, Jiang H, Chen X, Liang K. Comparative study on energy efficiency of low GWP refrigerants in domestic refrigerators with capacity modulation. Energy Build 2019;192:93–100. https://doi.org/10.1016/j.enbuild.2019.03.031.
[17] Aprea C, Greco A, Maiorino A. An experimental investigation on the substitution of HFC134a with HFO1234YF in a domestic refrigerator. Appl Therm Eng 2016;106:959–67. https://doi.org/10.1016/j.applthermaleng.2016.06.098.
[18] Illán-Gómez F, García-Cascales JR. Experimental comparison of an air-to-water refrigeration system working with R134a and R1234yf. Int J Refrig 2019;97:124–31. https://doi.org/10.1016/j.ijrefrig.2018.09.026.
[19] Colombo LPM, Lucchini A, Molinaroli L. Experimental analysis of the use of R1234yf and R1234ze(E) as drop-in alternatives of R134a in a water-to-water heat pump. Int J Refrig 2020;115:18–27. https://doi.org/10.1016/j.ijrefrig.2020.03.004.
[20] Lee Y, Jung D. A brief performance comparison of R1234yf and R134a in a bench tester for automobile applications. Appl Therm Eng 2012;35:240–2. https://doi.org/10.1016/j.applthermaleng.2011.09.004.
[21] Cho H, Lee H, Park C. Performance characteristics of an automobile air conditioning system with internal heat exchanger using refrigerant R1234yf. Appl Therm Eng 2013;61:563–9. https://doi.org/10.1016/j.applthermaleng.2013.08.030.
[22] Li W, Liu R, Liu Y, Wang D, Shi J, Chen J. Performance evaluation of R1234yf heat pump system for an electric vehicle in cold climate. Int J Refrig 2020;115:117–25. https://doi.org/10.1016/j.ijrefrig.2020.02.021.
[23] McLinden MO, Brown JS, Brignoli R, Kazakov AF, Domanski PA. Limited options for low-global-warming-potential refrigerants. Nat Commun 2017;8:14476. https://doi.org/10.1038/ncomms14476.
[24] Meng Z, Zhang H, Lei M, Qin Y, Qiu J. Performance of low GWP R1234yf/R134a mixture as a replacement for R134a in automotive air conditioning systems. Int J Heat Mass Transf 2018;116:362–70. https://doi.org/10.1016/j.ijheatmasstransfer.2017.09.049.
[25] Makhnatch P, Mota-Babiloni A, López-Belchí A, Khodabandeh R. R450A and R513A as lower GWP mixtures for high ambient temperature countries: Experimental comparison with R134a. Energy 2019;166:223–35. https://doi.org/10.1016/j.energy.2018.09.001.
[26] Morales-Fuentes A, Ramírez-Hernández HG, Méndez-Díaz S, Martínez-Martínez S, Sánchez-Cruz FA, Silva-Romero JC, et al. Experimental study on the operating characteristics of a display refrigerator phasing out R134a to R1234yf. Int J Refrig 2021;130:317–29. https://doi.org/10.1016/j.ijrefrig.2021.05.032.
[27] Mota-Babiloni A, Navarro-Esbrí J, Pascual-Miralles V, Barragán-Cervera Á, Maiorino A. Experimental influence of an internal heat exchanger (IHX) using R513A and R134a in a vapor compression system. Appl Therm Eng 2019;147:482–91. https://doi.org/10.1016/j.applthermaleng.2018.10.092.
[28] Velasco FJS, Illán-Gómez F, García-Cascales JR. Energy efficiency evaluation of the use of R513A as a drop-in replacement for R134a in a water chiller with a minichannel condenser for air-conditioning applications. Appl Therm Eng 2021;182. https://doi.org/10.1016/j.applthermaleng.2020.115915.
[29] Aprea C, Greco A, Maiorino A. HFOs and their binary mixtures with HFC134a working as drop-in refrigerant in a household refrigerator: Energy analysis and environmental impact assessment. Appl Therm Eng 2018;141:226–33. https://doi.org/10.1016/j.applthermaleng.2018.02.072.
[30] López-Belchí A. Assessment of a mini-channel condenser at high ambient temperatures based on experimental measurements working with R134a, R513A and R1234yf. Appl Therm Eng 2019;155:341–53. https://doi.org/10.1016/j.applthermaleng.2019.04.003.
[31] Thu K, Takezato K, Takata N, Miyazaki T, Higashi Y. Drop-in experiments and exergy assessment of HFC-32/HFO-1234yf/R744 mixture with GWP below 150 for domestic heat pumps. Int J Refrig 2021;121:289–301. https://doi.org/10.1016/j.ijrefrig.2020.10.009.
[32] Sun J, Li W, Cui B. Energy and exergy analyses of R513a as a R134a drop-in replacement in a vapor compression refrigeration system. Int J Refrig 2020;112:348–56. https://doi.org/10.1016/j.ijrefrig.2019.12.014.
[33] Khalid Shaker Al-Sayyab A, Mota-Babiloni A, Navarro-Esbrí J. Novel compound waste heat-solar driven ejector-compression heat pump for simultaneous cooling and heating using environmentally friendly refrigerants. Energy Conver Manage 2021;228:113703. https://doi.org/10.1016/j.enconman.2020.113703.
[34] Mota-Babiloni A, Mateu-Royo C, Navarro-Esbrí J, Barragán-Cervera Á. Experimental comparison of HFO-1234ze(E) and R-515B to replace HFC-134a in heat pump water heaters and moderately high temperature heat pumps. Appl Therm Eng 2021;196:117256. https://doi.org/10.1016/j.applthermaleng.2021.117256.
[35] Schulz M, Kourkoulas D. Regulation (EU) No 517/2014 of the European Parliament and of the Council of 16 April 2014 on fluorinated greenhouse gases and repealing Regulation (EC) No 842/2006. Off J Eur Union 2014;2014:L150/195-230.
[36] Al-Sayyab AKS, Navarro-Esbrí J, Mota-Babiloni A. Energy, exergy, and environmental (3E) analysis of a compound ejector-heat pump with low GWP refrigerants for simultaneous data center cooling and district heating. Int J Refrig 2022;133:61–72.
[37] ASHRAE. Standard 34, Designation and Safety Classification of Refrigerants. 2019.
[38] NIST Reference Fluid Thermodynamic and Transport Properties Database (REFPROP) 2018.
[39] Klein S. Engineering Equation Solver (EES) V10.2. Madison, USA: Fchart Software; 2020.
[40] Danfoss AS. Application guidelines Danfoss scroll compressors SM SY SZ. 2020.
[41] Khalifa AHN, Fataj JJ, Shaker AK. Performance study on a window type air conditioner condenser using alternative refrigerant R407C. Eng J 2017;21(1):235–43. https://doi.org/10.4186/ej.2017.21.1.235.
[42] European Standard EN 378-1. Refrigerating systems and heat pumps - safety and environmental requirements - Part 1: basic requirements, definitions, classification and selection criteria. 2016.